OPEN ACCESS
JOURNAL OF ADVANCED DIELECTRICS
Vol. 12, No. 2 (2022) 2250001 (6 pages)

DOI: 10.1142/S2010135X22500011

Enhanced piezoelectric properties in low-temperature sintering PZN–PZT ceramics by adjusting Zr/Ti ratio

Yaxia Luo, Tao Pu, Shibo Fan, Hong Liu* and Jianguo Zhu
College of Materials Science and Engineering, Sichuan University, Chengdu 610064, P. R. China
*liuh@scu.edu.cn

Received 4 January 2022; Revised 17 January 2022; Accepted 21 January 2022; Published 16 February 2022

$Pb_{0.96}Sr_{0.04}(Zr,Ti)_{0.7}(Zn_{1/3}Nb_{2/3})_{0.3}O_3$ (PZN–PZT) piezoceramics with various Zr/Ti ratios and Li_2CO_3 sintering aid were sintered at 900°C by the solid-state reaction route. The samples with different Zr/Ti ratios were compared according to microstructure, phase structure, piezoelectricity, ferroelectricity, and dielectric relaxation. The Zr/Ti ratio in the PZN–PZT ceramics greatly affects the electrical properties. The Zr/Ti ratio affects the proportion between the rhombohedral and tetragonal phases and also affects the grain size. The PZN–PZT ceramics with the Zr/Ti ratio of 53:47 have the largest grain size and have optimized piezoelectric properties (k_p = 0.58, d_{33} = 540 pC/N, and T_C = 250°C). The larger the grain size, the lesser the grain boundary, the easier the domain wall motion, and the better the piezoelectric properties. The PZT ceramic with Zr/Ti ratio of 53:47 locates the morphotropic phase boundary (MPB) region which is one of the key factors for the high piezoelectric properties of the PZT.

Keywords: Piezoelectric properties; ferroelectric properties; low-temperature sintering; PZT; MPB.

1. Introduction

PZT-based perovskite piezoceramics have been extensively produced and utilized as piezoelectric actuators and sensors because of their low cost and excellent performance.[1,2] PZT-based piezoceramics generally have coexistence of the tetragonal (*T*) and rhombohedral (*R*) phases near the morphotropic phase boundary (MPB) and have outstanding piezoelectric, dielectric, and ferroelectric properties, which originate from the coexistence of the tetragonal (*T*) and rhombohedral (*R*) phases. In addition, an intermediate monoclinic phase in the PZT-based perovskite piezoceramics near the MPB plays a key role in the improvement of the electrical properties.[3]

PZT-based piezoceramics are sintered at approximately 1200°C. Environmental pollution and nonstoichiometric ratio are caused by a large amount of PbO volatilize at this high temperature. To meet the requirements of commercialization and miniaturization for piezoelectric devices, the piezoceramic layers in a multilayer sheet need to be co-fired with the silver inner electrode layers below 900°C. Multilayer piezoceramics must use precious metals such as platinum or palladium as the internal electrodes at a high temperature of approximately 1200°C. Pure silver internal electrodes can be used at a low temperature less than 900°C, which greatly reduces the cost.[4,5] Lead-free Zn–Sn-based solder can be used to weld the conducting wire and components, which requires the piezoceramics with a Curie temperature (T_C) of more than 230°C.

$Pb(Zn_{1/3}Nb_{2/3})O_3$ with a T_C of 140°C is a typical ferroelectric relaxor, which has good electrical properties and has been broadly utilized as electromechanical devices.[5–8] The composite of the PZN–PZT piezoceramic system is a stable perovskite structure.[9,10] The PZN–PZT piezoceramics have attracted much attention.[11,12] Vittayakorn *et al.*[13] used a columbite method to synthesize 0.3PZN–0.7PZT(50/50) piezoceramics at a sintering temperature of 1225°C and achieved outstanding electrical properties (k_p = 0.70, d_{33} = 690 pC/N, and T_c = 299°C). Deng *et al.*[14] used a hot-pressing method to prepare 0.3PZN–0.7PZT(51/49) piezoceramics and obtained outstanding electrical properties (k_p = 0.70 and d_{33} = 845 pC/N). Chandarak *et al.*[15] concluded that the MPB composition for PZN–PZT(52/48) system is clearly at 0.3PZN–0.7PZT.

PZN–PZT piezoceramics with good piezoelectric properties have been sintered at low temperatures. Lee *et al.*[16] sintered MnO_2 doped 80% PZT(50/50)–20%PZN piezoceramics at 930°C and obtained outstanding electrical properties (k_p = 0.62, Q_m = 1000, and d_{33} = 330 pC/N). Ngamjarurojana *et al.*[17] sintered $0.04Pb(Ni_{1/3}Nb_{2/3})O_3$–$0.16Pb(Zn_{1/3}Nb_{2/3})O_3$–$0.8Pb(Zr_{0.48}Ti_{0.52})O_3$ piezoceramics at 900°C and obtained outstanding electrical properties (k_p = 0.56, Q_m = 1042, and d_{33} = 350 pC/N). Fan *et al.*[18] sintered 0.3PZN–0.7PZT(49/51)+Li_2CO_3+Sm_2O_3 piezoceramics at 900°C and achieved good piezoelectric properties (d_{33} = 483 pC/N, T_c = 394°C, and k_p = 0.65). Hou *et al.*[19] sintered $(Pb_{0.95}Sr_{0.05})(Zr_{0.50}Ti_{0.50})_{0.80}(Zn_{1/3}Nb_{2/3})_{0.20}O_3$+$MnO_2$ piezoceramics at 1000°C and obtained good piezoelectric properties (Q_m = 1360,

*Corresponding author.

k_p = 0.62, tanδ = 0.002, ε_r = 1240, T_c = 320°C, and d_{33} = 325 pC/N).

In this work, we prepared $Pb_{0.96}Sr_{0.04}(Zr_x,Ti_{1-x})_{0.7}$-$(Zn_{1/3}Nb_{2/3})_{0.3}O_3$ (PZN–PZT) piezoceramics with various Zr/Ti ratios and 0.30 wt.% Li_2CO_3 sintering aid at a low sintering temperature of 900°C by the traditional solid-reaction method. The Zr/Ti ratios were chosen as 49:51, 51:49, 53:47, 55:45, and 57:43, that is, x = 0.49, 0.51, 0.53, 0.55, and 0.57, respectively.

2. Experiments

The PZN–PZT piezoceramics were fabricated via the mixed-oxide powder route. The starting powders were reagent grade ZrO_2, PbO, TiO_2, $SrCO_3$, ZnO, Nb_2O_5, and Li_2CO_3. According to the stoichiometric ratios of the formula $Pb_{0.96}Sr_{0.04}(Zr_x,Ti_{1-x})_{0.7}(Zn_{1/3}Nb_{2/3})_{0.3}O_3$ +0.30 wt.% Li_2CO_3 (x = 0.49, 0.51, 0.53, 0.55, and 0.57), the powders were weighed and put into a pot for the ball milling for 11 h. The dried powder was calcined at 850°C for 3 h and then ball-milled for 20 h. The powder was added with an 8% polyvinyl-acetate binder after drying and pressed into discs. To remove the PVA binder, the disks were burned off at 650°C for 3.5 h. Then the disks were sintered at 900°C for 3 h. The sintered piezoceramics were coated with Ag pastes, fired at 720°C for 15 min. The piezoceramics were poled under a DC electric field of 30 kV/cm in silicone oil at 120°C.

The microstructure was observed using FE-SEM (JSM–7500F, JEOL, Japan). The phase structure was analyzed using X-ray diffraction (XRD) (X'Pert Pro MPD instrument, B.V. PANalytical, The Netherlands). The dielectric properties were analyzed by impedance meters (HP 4294A and HP 4980A, Agilent, USA). A ferroelectric test system (TF Analyzer 2000 E, aixACCT, Germany) was used to obtain the ferroelectric P–E loops. The quasi-static piezoelectric coefficient (d_{33}) was determined via a d_{33} meter (ZJ-3A, Institute of Acoustics, Chinese Academy of Sciences, China).

3. Results and Discussion

Figure 1 illustrates the room temperature XRD patterns in the 2θ range from 20° to 75° for the piezoceramics sintered at 900°C with various Zr/Ti ratios. All piezoceramics illustrate a perovskite structure, as shown in Fig. 1. Meantime, the typical splitting of diffraction peaks (002) and (200) indicates that the tetragonal phase exists in the piezoceramics. The splitting of the diffraction peaks of (200) and (002) becomes more obvious as the Zr/Ti ratio decreases from 57:43 to 49:51. Figure 2 shows the peak fitting around 45° for rhombohedral (R) and tetragonal (T) phases. The phase volume fraction for R and T phases can be calculated as[2]:

$$T \text{ phase fraction} = \frac{I_{(002)T} + I_{(200)T}}{I_{(002)T} + I_{(200)T} + I_{(200)R}} \times 100\%, \quad (1)$$

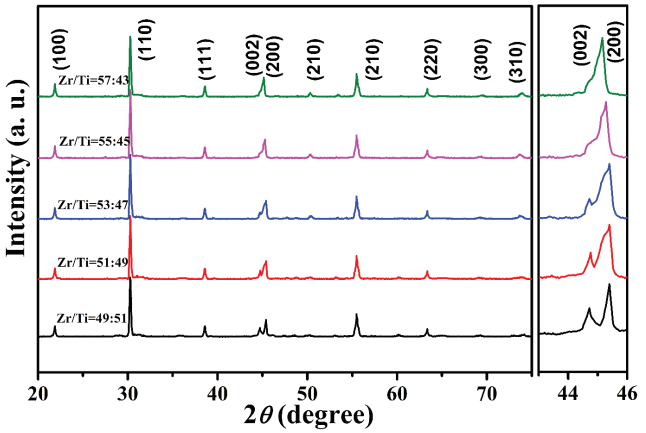

Fig. 1. XRD patterns for the piezoceramics with various Zr/Ti ratios.

where $I_{(200)R}$, $I_{(002)T}$, and $I_{(200)T}$ are the integrated intensities of the rhombohedral (200), tetragonal (002), and tetragonal (200) diffraction peaks, respectively. As can be seen from Fig. 2, when the Zr/Ti ratio is 49:51, the R phase volume fraction is about 30%, and when the Zr/Ti ratio exceeds 51:49, the R phase volume fraction increases sharply to about 70%.

Figures 3(a)–3(e) shows SEM images for the PZN–PZT piezoceramics with various Zr/Ti ratios. All samples show a uniform grain shape, as can be seen from the images. Figures 4(a)–4(e) shows the grain size distribution and Fig. 4(f) shows the average grain size for the PZN–PZT piezoceramics with different Zr/Ti ratios. The average grain size first increases to the maximum of 2.4 μm when the Zr/Ti ratio = 53:47 and then decreases. The PZT ceramic with Zr/Ti ratio of 53:47 locates the MPB region. At the MPB of a PZT, the energy difference between different phases is small enough, and the thermodynamic energy distribution is balanced.[20] The small energy difference between the rhombohedral phase and the tetragonal phase is conducive to the crystallization and ultimately leads to the larger grain size of PZT-based ceramics located in the MPB region than that of PZT-based ceramics deviating from the MPB region.

Figure 5 displays the piezoelectric properties for the PZN–PZT piezoceramics with different Zr/Ti ratios. Both planar electromechanical coupling coefficient (k_p) and piezoelectric coefficient (d_{33}) exhibit similar changing trends with the increased Zr/Ti ratio. The specimen with a Zr/Ti ratio of 53:47 has both k_p and d_{33} up to the maximum of 0.58 and 546 pC/N, respectively. However, the mechanical quality factor (Q_m) has an opposite changing trend to that of the d_{33} or k_p. The k_p and d_{33} have the same changing trends as the average grain size increases. The clamping effect of the grain boundary on the domain wall motion is greatly reduced due to the increased grain size, which facilitates the domain rotation and increases the piezoelectric properties.[21] The PZT ceramic with Zr/Ti ratio of 53:47 locates the MPB region. An intermediate monoclinic phase in the PZT-based perovskite

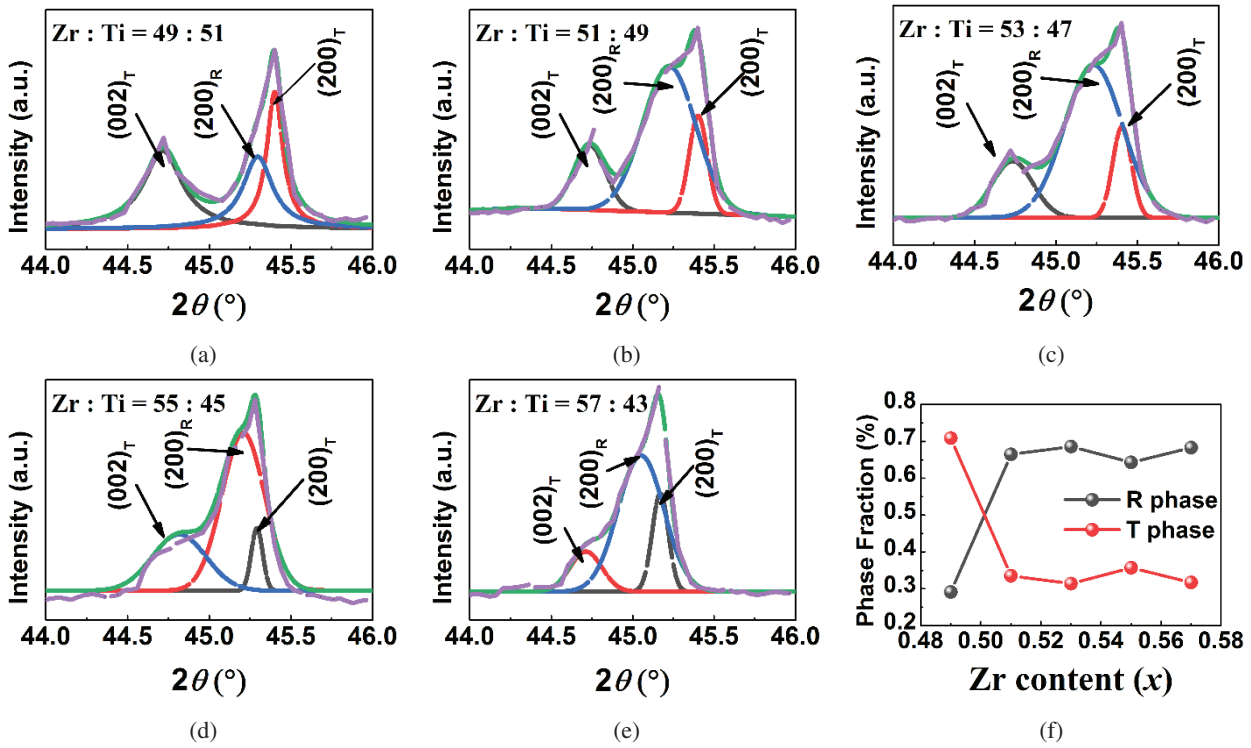

Fig. 2. (a)–(e) XRD patterns of the piezoceramics with various Zr/Ti ratios in the 2θ around 45°. *T* and *R* denote tetragonal and rhombohedral phases, respectively. (f) Phase volume fraction for *R* and *T* phases in the piezoceramics as a function of Zr/Ti ratio.

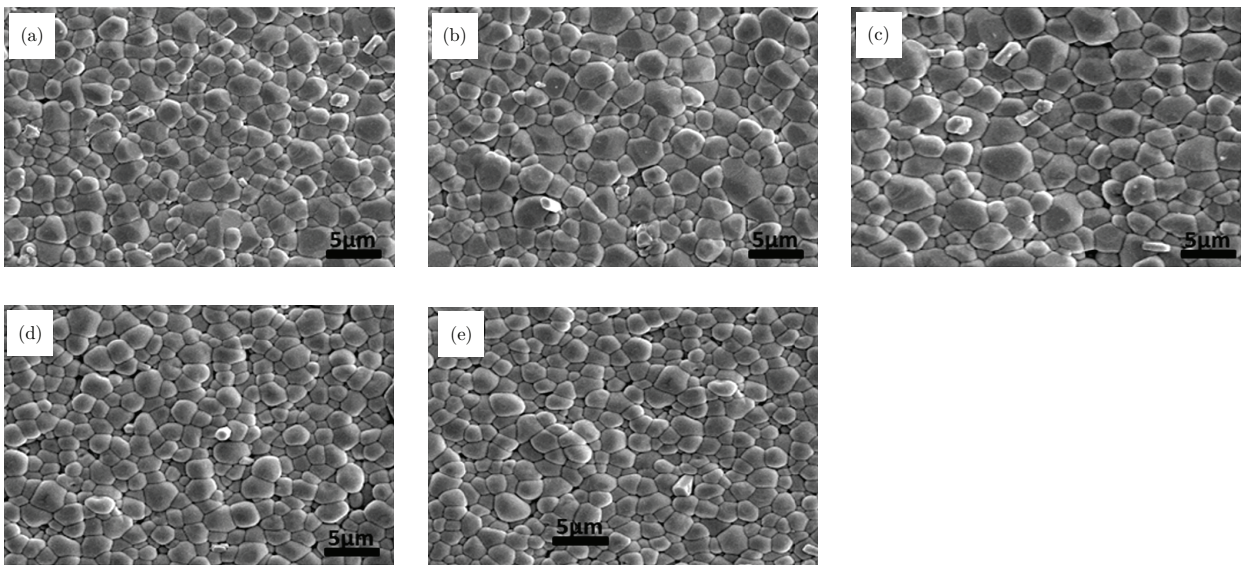

Fig. 3. SEM images for the piezoceramics with Zr/Ti ratios of (a) 49:51, (b) 51:49, (c) 53:47, (d) 55:45, and (e) 57:43.

piezoceramics near the MPB plays a key role in the improvement of the electrical properties.[3] The potential barriers between the rhombohedral phase and the tetragonal phase are small enough and play a dominant role. Therefore, polarization reorientation occurs easily even under small external stimuli (force, electric field, etc.) in the PZT ceramics.[22]

Figure 6 exhibits the dielectric loss ($\tan\delta$) and dielectric permittivity (ε_r) for the PZN–PZT piezoceramics with different Zr/Ti ratios measured at 1 kHz and 20°C. As shown in Fig. 6, the dielectric permittivity first increases to a maximum of 2500 then decreases as the Zr/Ti ratio increases, while the dielectric loss changes little. The enhancement of the dielectric permittivity may be due to the increased grain size, which causes the increased density.

Figures 7(a)–7(e) illustrates the temperature-dependent dielectric permittivity (ε_r) for the PZN–PZT piezoceramics

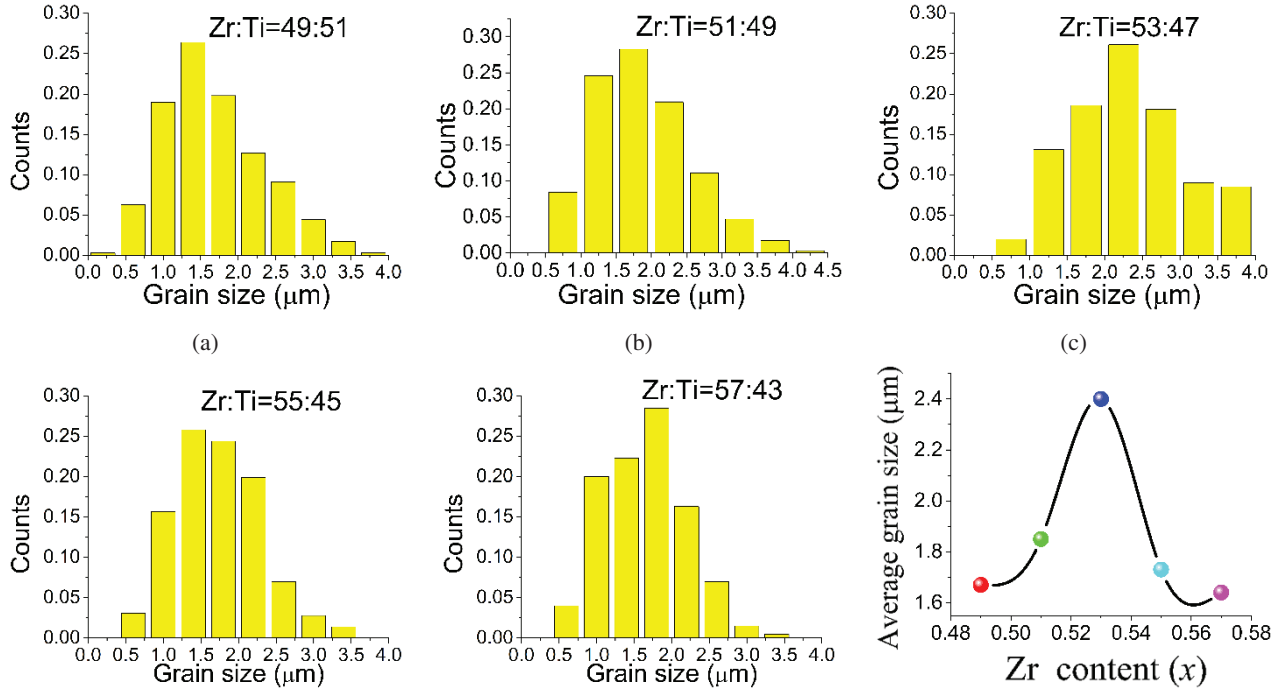

Fig. 4. Grain size distribution and average grain size for the piezoceramics with various Zr/Ti ratios.

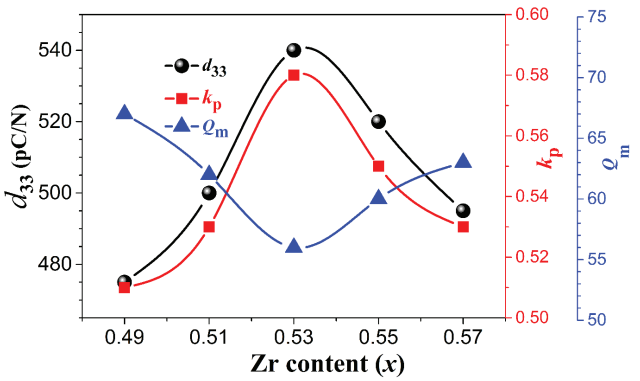

Fig. 5. Piezoelectric properties for the piezoceramics with various Zr/Ti ratios.

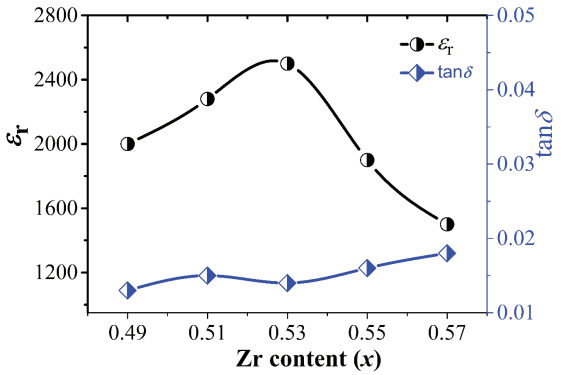

Fig. 6. Dielectric permittivity (ε_r) and loss (tanδ) for the piezoceramics with various Zr/Ti ratios.

with different Zr/Ti ratios measured at different frequencies (0.1, 1, 10, and 100 kHz). As observed in Figs. 7(c)–7(e) that weak and broad *R–T* phase transition peaks appear near 200°C. Only one main dielectric peak is observed for all samples, which is closely related to the paraelectric–ferroelectric phase transition. The dielectric peaks broaden, decrease and shift toward higher temperatures with the increased frequency which exhibits typical relaxor behaviors in the piezoceramics.[23–26] The Curie temperature (T_c) changes little as the Zr/Ti ratio increases. The relaxor behaviors originate from the temperature evolution and dynamic behaviors of nanoregions with the compositionally disordered crystals.[27]

Figure 7(f) illustrates the curves of $\ln(1/\varepsilon - 1/\varepsilon_{max})$ versus $\ln(T - T_{max})$ for the PZN–PZT piezoceramics with different Zr/Ti ratios measured at 1 kHz. The closer the γ value is to 2, the stronger the relaxation characteristics of the piezoceramics.[28] The γ fluctuates between 1.73 and 1.88, as can be seen from Fig. 7(f), all samples show the characteristics of ferroelectric relaxors.

Figure 8 depicts the ferroelectric *P–E* loops for the PZN–PZT piezoceramics with different Zr/Ti ratios. All *P–E* loops are saturated. The inset in Fig. 8 shows the E_c and P_r with the increased Zr/Ti ratio. The remanent polarization gradually increases to a maximum of 34.9 μC/cm^2 with a 53:47 Zr/Ti ratio, then gradually decreases. The remanent polarization has an opposite changing trend to that of the coercive field. The E_c reduces to a minimum of 0.79 kV/mm with a 53:47 Zr/Ti ratio. The results may be attributed to the increased grain size,

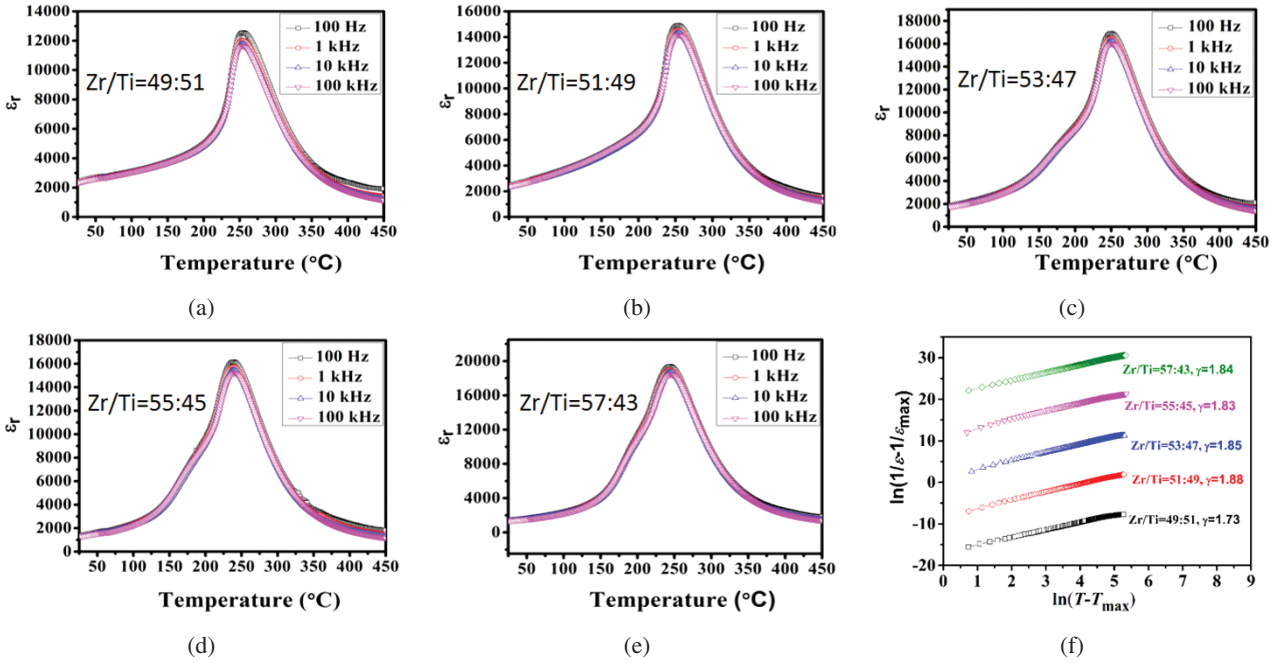

Fig. 7. (a)–(e) Temperature-dependent dielectric permittivity (ε_r) for the piezoceramics with various Zr/Ti ratios. (f) Curves of $\ln(1/\varepsilon-1/\varepsilon_{max})$ versus $\ln(T-T_{max})$ for the piezoceramics with various Zr/Ti ratios.

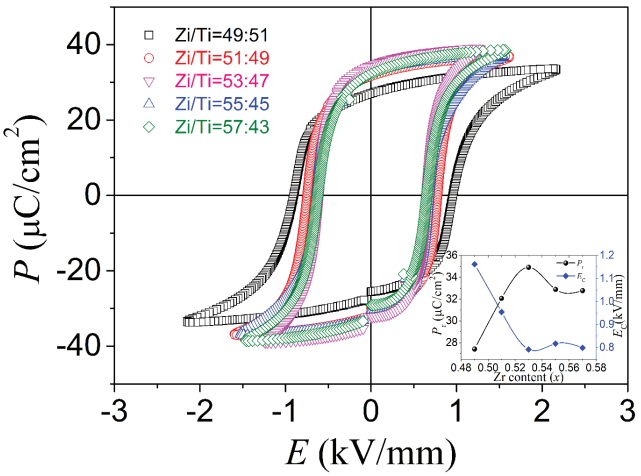

Fig. 8. *P–E* loops for the piezoceramics with various Zr/Ti ratios. The inset shows E_c and P_r for the piezoceramics with various Zr/Ti ratios.

which promotes the domain wall movement. High piezoelectric properties are because the domains rotate more easily.[29,30] As mentioned earlier, the PZT ceramic with Zr/Ti ratio of 53:47 locates the MPB region. The potential barriers between the rhombohedral phase and the tetragonal phase are small enough and cause easy polarization reorientation, thus leading to the high remanent polarization P_r and low coercive field E_c.

4. Conclusion

The PZN–PZT piezoceramics were sintered at 900°C. Optimized piez properties (k_p = 0.58, T_c = 250°C, d_{33} = 540 pC/N, Q_m = 56, ε_r = 2500, P_r = 34.9 μC/cm^2, and E_c = 0.79 kV/mm) were obtained in the sample with 53:47 Zr/Ti ratio. As the Zr/Ti ratio increases, the grain size first increases to a maximum and then gradually decreases. Most electrical properties such as d_{33}, k_p, and P_r show similar trends. The larger the grain size, the lesser the grain boundary, the easier the domain wall motion, and the better the piezoelectric properties.

Acknowledgments

This work was supported by Sichuan Science and Technology Program (2021YFG0234), the Fundamental Research Funds for the Central Universities (20826041E4280), and the National Natural Science Foundation of China (52032007).

References

[1]F. Li, S. Zhang, T. Yang, Z. Xu, N. Zhang, G. Liu, J. Wang, J. Wang, Z. Cheng, Z. G. Ye, J. Luo, T. R. Shrout and L. Q. Chen, The origin of ultrahigh piezoelectricity in relaxor-ferroelectric solid solution crystals, *Nat. Commun.* **7**, 13807 (2016), https://doi.org/10.1038/ncomms13807.

[2]R. Nie, Q. Zhang, Y. Yue, H, Liu, Y. Chen, Q. Chen, J. Zhu, P. Yu and D. Xiao, Phase structure–electrical property relationships in $Pb(Ni_{1/3}Nb_{2/3})O_3$–$Pb(Zr,Ti)O_3$-based ceramics, *J. Appl. Phys.* **119**, 124111 (2016), https://doi.org/10.1063/1.4945108.

[3]R. Guo, L. E. Cross, S. E. Park, B. Noheda, D. E. Cox and G. Shirane, Origin of the high piezoelectric response in $PbZr_{1-x}Ti_xO_3$, *Phys. Rev. Lett.* **84**, 5423 (2000), https://doi.org/10.1103/PhysRevLett.84.5423-5426.

[4]W. Zhang and R. E. Eitel, Sintering behavior, properties, and applications of co-fired piezoelectric/low-temperature co-fired

ceramic (PZT-SKN/LTCC) multilayer ceramics, *Int. J. Appl. Ceram. Technol*. **2**, 354 (2013), https://doi.org/10.1111/j.1744-7402.2011.02747.x.

[5]J. J. Choi, J. H. Lee, B. D. Hahn, W. H. Yoon and D. S. Park, Co-firing of PZN-PZT/Ag multilayer actuator prepared by tape-casting method, *Mater. Res. Bull*. **43**, 483 (2008), https://doi.org/10.1016/j.materresbull.2007.02.033.

[6]Y. Yue, Y. Hou, M. Zheng, X. Yan and M. Zhu, Submicron crystalline buildup and size-dependent energy harvesting characteristic in PZN–PZT ternary ferroelectrics, *J. Am. Ceram. Soc*. **100**, 5211 (2017), https://doi.org/10.1111/jace.15054.

[7]J. Lou, M. Liu, D. Reed, Y. Ren and N. X. Sun, Giant electric field tuning of magnetism in novel multiferroic FeGaB/Lead Zinc Niobate–Lead Titanate (PZN–PT) Heterostructures, *Adv. Mater.* **21**, 4711 (2009), https://doi.org/10.1002/adma.200901131.

[8]N. Vittayakorn, G. Rujijanagul, X. Tan, H. He, M. A. Marquardt and D. P. Cann, Dielectric properties and morphotropic phase boundaries in the xPb$(Zn_{1/3}Nb_{2/3})O_3$–$(1–x)$Pb$(Zr_{0.5}Ti_{0.5})O_3$ pseudo-binary system, *J. Electroceram.* **16**, 141 (2006), https://doi.org/10.1007/s10832-006-4927-2.

[9]H. Fan and H. E. Kim, Perovskite stabilization and electromechanical properties of polycrystalline lead zinc niobate-lead zirconate titanate, *J. Appl. Phys*. **91**, 317 (2002), https://doi.org/10.1063/1.1421036.

[10]M. Zheng, Y. Hou, M. Zhu, M. Zhang and H. Yan, Shift of morphotropic phase boundary in high-performance fine-grained PZN–PZT ceramics, *J. Eur. Ceram. Soc*. **34**, 2275 (2014), https://doi.org/10.1016/j.jeurceramsoc.2014.02.041.

[11]Z. Yang, H. Li, X. Zong and Y. Chang, Structure and electrical properties of PZT–PMS–PZN piezoelectric ceramics, *J. Eur. Ceram. Soc*. **26**, 3197 (2006), https://doi.org/10.1016/j.jeurceramsoc.2005.08.005.

[12]X. Zeng, A. L. Ding, T. Liu, G. C. Deng, X. S. Zheng and W. X. Cheng, Excess ZnO addition in pure and La-substituted PZN–PZT ceramics, *J. Am. Ceram. Soc*. **89**, 728 (2006), https://doi.org/10.1111/j.1551-2916.2005.00754.x.

[13]N. Vittayakorn, G. Rujijanagul, X. Tan, H. He, M. A. Marquardt and D. P. Cann, Dielectric properties and morphotropic phase boundaries in the xPb$(Zn_{1/3}Nb_{2/3})O_3$–$(1–x)$Pb$(Zr_{0.5}Ti_{0.5})O_3$ pseudo-binary system, *J. Electroceram*. **16**, 141 (2006), https://doi.org/10.1007/s10832-006-4927-2.

[14]G. C. Deng, Q. R. Yin, A. L. Ding, X. S. Zheng, W. X. Cheng and P. S. Qiu, High piezoelectric and dielectric properties of La-Doped $0.3Pb(Zn_{1/3}Nb_{2/3})O_3$–$0.7Pb(Zr_xTi_{1-x})O_3$ ceramics near morphotropic phase boundary, *J. Am. Ceram. Soc.* **88**, 2310 (2005), https://doi.org/10.1111/j.1551-2916.2005.00391.x.

[15]S. Chandarak, M. Unruan, A. Prasatkhetragarn and R. Yimnirun, Structural investigation of PZT–PNN and PZT–PZN probed by synchrotron X-ray absorption spectroscopy, *Ferroelectrics* **455**, 117 (2013), https://doi.org/10.1080/00150193.2013.845485.

[16]S. M. Lee, S. H. Lee, C. B. Yoon, H. E. Kim and K. W. Lee, Low-temperature sintering of MnO_2-doped PZT–PZN Piezoelectric ceramics, *J. Electroceram*. **18**, 311 (2007), https://doi.org/10.1007/s10832-007-9174-7.

[17]A. Ngamjarurojana, S. Ural, S. H. Park, S. Ananta, R. Yimnirun and K. Uchino, Piezoelectric properties of low-temperature sintering in $Pb(Zr,Ti)O_3$–$Pb(Zn,Ni)_{1/3}Nb_{2/3}O_3$ ceramics for piezoelectric transformer applications, *Ceram. Int.* **34**, 705 (2008), https://doi.org/10.1016/j.ceramint.2007.09.012.

[18]G. F. Fan, M. B. Shi, W. Z. Lu, Y. Q. Wang and F. Liang, Effects of Li_2CO_3 and Sm_2O_3 additives on low-temperature sintering and piezoelectric properties of PZN–PZT ceramics, *J. Eur. Ceram. Soc*. **34**, 23 (2014), https://doi.org/10.1016/j.jeurceramsoc.2013.07.028.

[19]Y. D. Hou, M. K. Zhu, H. Wang, B. Wang, H. Yan and C. S. Tian, Piezoelectric properties of new MnO_2-added 0.2 PZN–0.8 PZT ceramic, *Mater. Lett*. **58**, 1508 (2004), https://doi.org/10.1016/j.matlet.2003.10.013.

[20]H. J. Liu, H. J. Wu, K. P. Ong, T. N. Yang, P. Yang, P. K. Das, X. Chi, Y. Zhang, C. Z. Diao, W. K. A. Wong, E. P. Chew, Y. F. Chen, C. K. I. Tan, A. Rusydi, M. B. H. Breese, D. J. Singh, L. Q. Chen, S. J. Pennycook and K. Yao, Giant piezoelectricity in oxide thin films with nanopillar structure, *Science* **369**, 292 (2020), https://10.1126/science.abb3209.

[21]Y. D. Hou, L. M. Chang, M. K. Zhu, X. M. Song and H. Yan, Effect of Li_2CO_3 addition on the dielectric and piezoelectric responses in the low-temperature sintered 0.5PZN–0.5PZT systems, *J. Appl. Phys*. **102**, 084507 (2007), https://doi.org/10.1063/1.2800264.

[22]Y. Chen, X. J. Xu, W. Ali, Y. J. Wang, Y. P. Wang, Y. Yang, L. Chen and G. L. Yuan, Piezoelectricity in Excess of 800 pC/N over 400°C in $BiScO_3$– $PbTiO_3$–$CaTiO_3$ Ceramics, *ACS Appl. Mater. Interfaces* **13**, 33253 (2021), https://doi.org/10.1021/acsami.1c07492.

[23]M. R. Suchomel and P. K. Davies, Enhanced tetragonality in xPbTiO_3–$(1–x)$Bi$(Zn_{1/2}Ti_{1/2})O_3$ and related solid solution systems, *Appl. Phys. Lett*. **86**, 262905 (2005), https://doi.org/10.1063/1.1978980.

[24]J. Kelly, M. Leonard, C. Tantigate and A. Safari, Effect of composition on the electromechanical properties of $(1–x)$Pb$(Mg_{1/3}Nb_{2/3})O_3$–xPbTiO_3 Ceramics, *J. Am. Ceram. Soc*. **80**, 957 (1997), https://doi.org/10.1111/j.1151-2916.1997.tb02927.x.

[25]Y. Yue, Q. Zhang, R. Nie, H. Liu, Q. Chen, P. Yu, J. Zhu and D. Xiao, Influence of sintering temperature on phase structure and electrical properties of $0.55Pb(Ni_{1/3}Nb_{2/3})O_3$–$0.45Pb(Zr_{0.3}Ti_{0.7})O_3$ ceramics, *Mater. Res. Bull*. **92**, 123 (2017), https://doi.org/10.1016/j.materresbull.2017.04.015.

[26]J. Su, X. Lu, Y. Liu, J. Zhang, G. Li, X. Ruan, F. Huang, J. Du and J. Zhu, Multiferroicity in $0.7Pb(Zr_{0.52}Ti_{0.48})O_3$–$0.3Pb(Ni_{1/3}Nb_{2/3})O_3$ ceramics, *Appl. Phys. Lett*. **100**, 102905 (2012), https://doi.org/10.1063/1.3693145.

[27]C. H. Wang, The piezoelectric and dielectric properties of PZT–PMN–PZN, *Ceram. Int*. **30**, 605 (2004), https://doi.org/10.1016/j.ceramint.2003.07.005.

[28]H. Liu, R. Nie, Y. Yue, Q. Zhang, Q. Chen, J. Zhu, P. Yu, D. Xiao, C. Wang and X. Wang, Effect of MnO_2 doping on piezoelectric, dielectric and ferroelectric properties of PNN–PZT ceramics, *Ceram. Int*. **41**, 11359 (2015), https://doi.org/10.1016/j.ceramint.2015.05.094.

[29]H. Liu, J. Chen, L. Fan, Y. Ren, Z. Pan, K. V. Lalitha, J. Rodel and X. Xing, Critical role of monoclinic polarization rotation in high-performance perovskite piezoelectric materials, *Phys. Rev. Lett.* **119**, 017601 (2017), https://doi.org/10.1103/PhysRevLett.119.017601.

[30]H. Chen, J. Xing, J. Xi, T. Pu, H. Liu and J. Zhu, Phase, domain, and microstructures in Sr^{2+} substituted low-temperature sintering PZT-based relaxor ferroelectrics, *J. Am. Ceram. Soc.* **104**, 6266 (2021), https://doi.org/10.1111/jace.17989.